

Cell-Penetrating Peptides, Electroporation, and Drug Delivery

Kevin Cahill
cahill@unm.edu

May 30, 2022

Biophysics Group, Department of Physics & Astronomy, University of New Mexico, Albuquerque, NM 87131

ABSTRACT Certain short polycations, such as TAT and oligoarginine, rapidly pass through the plasma membranes of mammalian cells by a mechanism called transduction, as well as by endocytosis and macropinocytosis. These cell-penetrating peptides (CPPs) can carry with them cargos of 30 amino acids, more than the nominal limit of 500 Da and enough to be therapeutic. An analysis of the electrostatics of a charge outside the cell membrane and some recent experiments suggest that transduction may proceed by molecular electroporation. Ways to target diseased cells, rather than all cells, are discussed.

I. THE PROBLEM OF DRUG DELIVERY

We could cure cancer if we knew how to deliver a drug intact to the cytosol of every cancer cell, sparing healthy cells. The circulatory system can deliver a drug to every cell in the body, and certain chemical tricks protect drugs from peptidases [1] and nucleases [2]. But it's harder to cope with antibodies, spare healthy tissues, and get drugs past the plasma membrane, which blocks or endocytoses molecules in excess of 500 Da [3].

This paper is about cell-penetrating peptides and other cations that can overcome the 500-Da restriction barrier and about tricks that may spare healthy cells. Section II describes several cell-penetrating peptides (CPPs), and section III sketches a variety of therapeutic applications of CPPs. Section IV reviews basic facts about the lipid bilayer of the eukaryotic cell. New work on the electrostatics of the bilayer is presented in section V. Section VI sketches a model [4, 5] of the transduction of polyarginine and mentions some experimental support [6] which the model has recently received. Section VII discusses a broader class of cell-penetrating molecules and suggests ways to target cancer cells.

II. CELL-PENETRATING PEPTIDES

In 1988, two groups [7, 8] working on HIV reported that the **trans-activating transcriptional activator (TAT)** of HIV-1 can cross cell membranes. The engine driving this 86-aa cell-penetrating peptide (CPP) is residues 48–57 GRKKRRQRRR which carry a charge of $+8e$. Other CPPs were soon found. Antp (aka Penetratin, PEN) is residues 43–58 RQIKIWFQNRRMKWKK of Antennapedia, a homeodomain of the fly; it carries a charge of $+7e$. The polyarginine R^n carries charge $+ne$, where often $n = 7, 8, \text{ or } 9$. Other CPPs have been discovered (VP22) or synthesized (transportan). The structural protein VP22 of the tegument of herpes simplex virus type 1 (HSV-1) has charge $+15e$. Transportan GWTLNSAGYLLG-K-INLKALAALAKKIL-amide is a chimeric peptide constructed from the 12 N-terminal residues of galanin in the N-terminus with the 14-residue sequence of mastoparan and a connecting lysine [9]. With its ter-

minal amide group, its charge is $+5e$.

These and other short, positively charged peptides can penetrate the plasma membranes of live cells and can tow along with them cargos that greatly exceed the 500 Da restriction barrier. They are promising therapeutic tools when towing cleverly chosen peptide cargos of from 8 to 33 amino acids [10–22].

Many early experiments on CPPs were wrong because the cells were fixed or insufficiently washed. Even careful experiments sometimes have yielded inconsistent results—in part because fluorescence varies with the (sub)cellular conditions and the fluorophores [23].

Yet some clarity is emerging: TAT carries cargos across cell membranes with high efficiency by at least two functionally distinct mechanisms according to whether the cargo is big or small [24]. Big cargos, such as proteins or quantum dots, enter via caveolae endocytosis and macropinocytosis [25, 26], and relatively few escape the cytoplasmic vesicles in which they then are trapped [24].

Small cargos, such as peptides of fewer than 30–40 amino acids, enter both slowly by endocytosis and rapidly by transduction with direct access to the cytosol, an unknown mechanism that uses the membrane potential [24, 27–30]. Peptides fused to TAT enter cells within seconds [31].

It remains unclear how big cargos aided by several CPPs enter cells [32]. For instance, superparamagnetic nanoparticles encased in aminated dextran and attached to 45 tat peptides are thought to enter cells by adsorptive endocytosis [33–35] but they do enter slowly at 4°C [36].

III. THERAPEUTIC APPLICATIONS

The use of a cell-penetrating peptide (CPP) to carry into cells a biologically active peptide of up to some 35 amino acids (aa) allows for $20^{35} = 3 \times 10^{45}$ different peptides and may lead to strikingly smart drugs, some of which may selectively target tumor cells [10]. I will now briefly describe 11 promising advances toward this goal of cell-penetrating-peptide drugs (CPPDs).

The CXC chemokine receptor 4 (CXCR4) is over-expressed in > 20 types of cancer, including prostate, breast, colon, and small-cell lung cancer. Snyder *et*

al. [11] attached the CXCR4 ligand DV3 to the CPP TAT and then either to a Cdk2-antagonist peptide (DV3-TAT-RxL) or to a p53-activating peptide (DV3-{TAT-p53C'}_{ri}) in which *ri* means retroinverso [1]. The DV3+RxL and DV3+p53C' cargoes respectively consisted of 19 and 33 aa. Both ligand-guided CPPs were more than twice as effective as unguided CPPs in killing CXCR4 expressing Namalwa lymphoma cells.

The transcription factor hypoxia-inducible factor-1 (HIF), a master regulator of the hypoxic response, is itself regulated thru the oxygen-dependent degradation domains (ODD) of its α -chains (HIF α). The NODD and CODD peptides respectively are the amino- and carboxyl-terminal sequences of ODD. Pugh *et al.* injected TAT fused to CODD (tat-CODD) into sponges implanted subcutaneously (s.c.) in mice. After 7 days, they found that tat-CODD but not the control mutant tat-CODD^{mut} produced blood vessels of increasing density and complexity [12]. Their results for tat-NODD were similar. Thus TAT delivery of NODD and CODD peptides can stimulate angiogenesis and may lead to therapies for ischemic diseases. The cargoes NODD and CODD respectively were 28 and 19 aa long.

If the DNA-binding ability of the transcription factor E2F1 is not curtailed as cells traverse and prepare to exit S phase, then apoptosis is likely. In normal cells, the retinoblastoma tumor-suppressor protein pRB converts E2Fs from activators to repressors of transcription. But pRB often is not present in transformed cells. Cyclin A/cdk2 also neutralizes E2F1's DNA-binding ability. So if one blocked the interaction of cyclin A/cdk2 and E2F1 in cells, then the transcription factor E2F1 would continue to activate transcription after exit from S phase in cancer cells but not in normal cells equipped, as they are, with pRB. Apoptosis then would occur in the transformed cells but not in the normal ones. Chen *et al.* [13] used TAT and PEN to carry the synthetic peptides PVKRRFLG and PVKRRDL, which block the interaction of cyclin A/cdk2 and E2F1, into U2OS osteosarcoma cells, T-antigen-transformed WI38/VA13 cells, and healthy WI38 cells. They found that apoptosis occurred in and only in the cancer cells [13]. Both cargoes were 8 aa long.

The CPPD PEN-PVKRRDL injected in and near tumors in nude mice that had been s.c. injected with SVT2 cells with altered cyclin D/Rb pathways produced large areas of apoptosis and necrosis, particularly at the tumor periphery [14]. PEN-PVKRRFLG had similar effects on hereceptin-resistant mammary tumors from HER2 transgenic mice implanted in syngeneic FVB mice [14]. Both cargoes were 8 aa long.

HDM2 binds and inhibits p53, keeping it at low levels in normal cells. Oncogenic mutations disrupt this HDM2-p53 equilibrium, allowing p53 to accumulate and induce stasis or apoptosis. In most cancer cells, p53 is mutated or HDM2 is overexpressed. Uveal melanomas (common eye cancers in adults) overexpress HDM2. A peptide that blocks HDM2 may liberate p53, which may

induce apoptosis in cancer cells but remain inactive in normal ones. The sequence QETFSDLWKLIP (α HDM2) of the p53 binding site for HDM2 blocks HDM2. TAT-G- α HDM2 at concentrations of 200–300 μ M induces apoptosis in MM-23, MM-24, & MM-26 uveal, Y79 & WERI retinoblastoma, U2OS osteosarcoma, and C33A cervical cancer cells with little effect on normal cells [15]. Injection of 10⁷ WERI human retinoblastoma cells produced intraocular tumors in the anterior chambers of rabbit eyes. But the injection of TAT- α HDM2 (intraocular concentration 200 μ M) began to dissolve the tumors into a fine cloud within 24 hours. A second injection reduced the viable tumor mass by 76% within 72 hours with no histologic damage to other ocular tissues. The cargo was 13 aa long.

The CPP RRQRRTSKLMKR (“PTD-5,” charge +7e) joined to the antimicrobial peptide KLAKLAKKLAKLAK (“KLA”) with a diglycine spacer forms the pro-apoptotic peptide PTD-5-GG-KLA (“DP1”). Robbins *et al.* injected 50 μ L of 1 mM DP1 or KLA for 11 days into C57BL/6 mice with single-flank, day-12 MCA205 fibrosarcomas. After only 8 days of treatment, DP1 but not KLA had shrunk the tumors. DP1 but not KLA or PTD-5 activated caspase-3 and mediated apoptosis [16]. The cargo was 16 aa.

Renal-cell cancer (RCC) is the seventh most common and is resistant to non-surgical therapies. Sporadic clear-cell renal cancer often exhibits functional inactivation of the protein pVHL of the von-Hippel-Lindau (VHL) gene. Residues 104–123 of a β -sheet of pVHL inhibits the IGF-I signaling upon which RCC is dependent [17]. Daily intraperitoneal injections of 2 nmol of TAT-FLAG-pVHL(104–123) arrested and then reduced tumors of 786-O RCC cells in nude mice, while TAT-FLAG had no effect. (FLAG is the antigen YKDDDDK.) The cargo was 27 aa long.

The tumor-suppressor gene 16INK4A often is inactivated by intragenic mutation, homozygous deletion, or methylation silencing in many human cancers, especially pancreatic cancer. Its protein p16 inhibits the phosphorylation of Rb by cdk-4 and by cdk-6, and so p16 blocks the G₁→S phase transition. Residues 84–103 of p16 are sufficient to block this transition. The Trojan p16 peptide was p16(84–103)C linked by a disulfide bond to C-Antp: DAAREGFLDTLVVLRHAGARC-CRQIKIWFQNRRMKWKK. Trojan p16 (i.p. 100 μ g/mouse/day) reduced AsPC-1 and BxPC-3 s.c. tumors respectively by factors of 2 and 5 without hematological cytotoxicity or body weight loss [18]. The cargo was 22 aa long.

The DOC-2/DAB2 (differentially expressed in ovarian cancer-2/disabled 2) protein often is lost in prostate cancer. As part of the homeostatic machinery in the normal prostate epithelium, DOC-2/DAB2 modulates the Grb2-SOS-MAPK signal axis. The small peptide FQLRQPPLVPSRKGE is less immunogenic than the protein DOC-2/DAB2 but still has some of its ability to interact with SH3 domains. Hsieh *et al.* used the CPP R11

to carry this peptide into cells. The CPPD R¹¹-GGG-FQLRQPPLVPSRKGE at 5 μ M for 3 hours inhibited the growth of LNCaP and C4-2 prostate-cancer cells. [19] The cargo was 18 aa long.

The peptide p53C', derived from the K-rich C-terminal domain of p53, activates specific DNA binding by p53, activates wild-type p53, restores function to several p53 contact mutants, and induces apoptosis or G₁ growth arrest in cancer cells but not in normal ones [20]. The retro-inverso [1] D-isomer TAT-p53C'_{ri} **rrrqrrkkrgygkkhrstsggkksklhshsarg** resists proteolysis better than the L-isomer p53C'-TAT. TAT-p53C'_{ri} induces G₁ cell-cycle arrest and senescence better than p53C'-TAT in murine TA3/St mammary cancer cells, which express wild-type p53, and induces the transcription of p53 from a wild-type p53 expression vector in p53-null, H1299 lung-cancer cells [20]. Injections (i.p.) of 600 μ g of TAT-p53C'_{ri} once a day for 12 days inhibited solid-tumor growth in mice and led to a 6-fold increase in longevity in mice with terminal peritoneal carcinomatosis. Sixteen injections (i.p.) of 900 μ g of TAT-p53C'_{ri} over 20 days cured 50% of mice with terminal peritoneal lymphoma [20]. The cargo was 23 aa long.

Residues 1–15 of the human ventricular myosin light chain-1 (VLC-1) binds to actin, targets the actin/MLC-1 interaction, and improves the contraction of isolated perfused hearts [21]. VLC-1 fused to TAT entered adult cardiomyocytes with high efficiency, accumulated in the actin-containing I-band of their sarcomeres, and enhanced their contractility without changing their myoplasmic Ca²⁺ levels [22]. The cargo was 15 aa long.

In these transduction experiments, the heaviest cargo was 33 amino acids. In my somewhat casual literature search, I found no biomedical articles describing the transduction of heavier cargoes. In the biophysical experiments, the cargoes respectively were 20, 22, and 26 aa (apart from a tiny rhodamine tag) [24], and just a \sim 400 Da fluorophore [37].

IV. MAMMALIAN PLASMA MEMBRANES

The plasma membrane of a mammalian cell is a lipid bilayer that is 4 or 5 nm thick. Of the four main phospholipids in it, three—phosphatidylethanolamine (PE), phosphatidylcholine (PC), and sphingomyelin (SM)—are neutral, and one, phosphatidylserine (PS), is negatively charged. In live cells, PE and PS are mostly in the cytosolic layer, and PC and SM in the outer layer [38, 39]. Aminophospholipid translocase (flippase) moves PE and PS to the inner layer; floppase slowly moves all phospholipids to the outer layer [38].

Glycolipids make up about 5% of the lipid molecules of the outer layer of a mammalian plasma membrane where they may form lipid rafts. Their hydrocarbon tails normally are saturated. Instead of a modified phosphate group, they are decorated with galactose, glucose, GalNAc = N-acetylgalactosamine, and other sugars. The

most complex glycolipids—the gangliosides—have negatively charged sialic-acid (NANA) groups.

A living cell maintains an electrostatic potential of between 20 and 120 mV across its plasma membrane. The electric field E within the membrane points into the cell and is huge, about 15 mV/nm or 1.5×10^7 V/m if the potential difference is 60 mV across a membrane of 4 nm. Conventionally, one reports membrane potentials as the electric potential inside the cell minus that outside, so that here $\Delta V = -60$ mV. Near but outside the membrane, this electric field falls-off exponentially $E(r) = E \exp(-r/D_\ell)$ with the ratio of the distance r from the membrane to the Debye length D_ℓ , which is of the order of a nanometer. The rapid entry of TAT fused to peptides is frustrated only by agents that destroy the electric field E [24].

Most of the phospholipids of the outer leaflet of the plasma membrane are neutral PCs & SMs. They vastly outnumber the negatively charged gangliosides, which are a subset of the glycolipids, which themselves amount only to 5% of the outer layer. Imagine now that polyarginine-cargo molecules are in the extra-cellular environment. Many of them will be pinned down by the electric field $E(r)$ just outside the membrane, their positively charged guanidinium groups interacting with the negative phosphate groups of neutral dipolar PC & SM head groups [29]. (Other CPP-cargo molecules will stick to negatively charged gangliosides and to glycosaminoglycans (GAGs) attached to transmembrane proteoglycans (PGs); these slowly will be endocytosed. PGs with heparan-sulfate GAGs are needed for TAT-protein endocytosis [40].) It is crucial that the dipolar PC & SM head groups are neutral and so do not cancel or reduce the positive electric charge of a CPP-cargo molecule. The net positive charge of a CPP-cargo molecule and the negatively charged PSs under it on the inner leaflet form a kind of capacitor.

V. MEMBRANE ELECTROSTATICS

A recent calculation [4] of the electrostatic potential due to a charge outside the phospholipid bilayer of a eukaryotic cell shows how effectively this plasma membrane insulates the cell from external charges.

The electrostatic potential in the lipid bilayer $V_\ell(\rho, z)$ due to a charge q at the point $(0, 0, h)$ on the z -axis, a height h above the interface between the lipid bilayer and the extra-cellular environment, is

$$V_\ell(\rho, z) = \frac{q}{4\pi\epsilon_0\epsilon_{w\ell}} \sum_{n=0}^{\infty} (pp')^n \left(\frac{1}{\sqrt{\rho^2 + (2nt + h - z)^2}} - \frac{p'}{\sqrt{\rho^2 + (2(n+1)t + h + z)^2}} \right) \quad (1)$$

in which t is the thickness of the lipid bilayer, $\epsilon_{w\ell} = (\epsilon_w + \epsilon_\ell)/2$ is average of the relative permittivities of the

extra-cellular fluid ϵ_w and the lipid bilayer ϵ_ℓ , and p and p' are the ratios

$$p = \frac{\epsilon_w - \epsilon_\ell}{\epsilon_w + \epsilon_\ell} \quad \text{and} \quad p' = \frac{\epsilon_c - \epsilon_\ell}{\epsilon_c + \epsilon_\ell} \quad (2)$$

which lie between 0 and 1, ϵ_c being the relative permittivity of the cytosol [4]. The potential in the extra-cellular medium is

$$V_w(\rho, z) = \frac{q}{4\pi\epsilon_0\epsilon_w} \left(\frac{1}{r} + \frac{p}{\sqrt{\rho^2 + (z+h)^2}} - \frac{\epsilon_w\epsilon_\ell}{\epsilon_w^2} \sum_{n=1}^{\infty} \frac{p^{n-1}p'^n}{\sqrt{\rho^2 + (z+2nt+h)^2}} \right) \quad (3)$$

in which $r = \sqrt{\rho^2 + (z-h)^2}$ is the distance from the charge q [4]. The potential in the cytosol due to the same charge q is

$$V_c(\rho, z) = \frac{q\epsilon_\ell}{4\pi\epsilon_0\epsilon_w\epsilon_\ell\epsilon_c} \sum_{n=0}^{\infty} \frac{(pp')^n}{\sqrt{\rho^2 + (2nt+h-z)^2}}. \quad (4)$$

where $\epsilon_{\ell c}$ is the mean relative permittivity $\epsilon_{\ell c} = (\epsilon_\ell + \epsilon_c)/2$ [4].

If one seeks the potential only directly above or below the charge, that is, for $\rho = 0$, then these formulas become simpler and may be expressed in terms of the Lerch transcendent

$$\Phi(z, s, \alpha) = \sum_{n=0}^{\infty} \frac{z^n}{(n+\alpha)^s}. \quad (5)$$

For $\rho = 0$, the potential is

$$\begin{aligned} V_\ell(0, z) &= \frac{q}{4\pi\epsilon_0\epsilon_w\ell} \sum_{n=0}^{\infty} (pp')^n \left(\frac{1}{2nt+h-z} - \frac{p'}{2(n+1)t+h+z} \right) \\ &= \frac{q}{8\pi\epsilon_0\epsilon_w\ell t} \left[\Phi\left(pp', 1, \frac{h-z}{2t}\right) - p' \Phi\left(pp', 1, 1 + \frac{h+z}{2t}\right) \right] \end{aligned} \quad (6)$$

in the lipid bilayer,

$$V_w(0, z) = \frac{q}{4\pi\epsilon_0\epsilon_w} \left[\frac{1}{|z-h|} + \frac{p}{z+h} - \frac{\epsilon_w\epsilon_\ell}{\epsilon_w^2 p} \left(\frac{1}{2t} \Phi\left(pp', 1, \frac{z+h}{2t}\right) - \frac{1}{z+h} \right) \right] \quad (7)$$

in the extracellular environment, and

$$V_c(0, z) = \frac{q\epsilon_\ell}{8\pi\epsilon_0\epsilon_w\ell\epsilon_{\ell c}t} \Phi\left(pp', 1, \frac{h-z}{2t}\right). \quad (8)$$

in the cytosol.

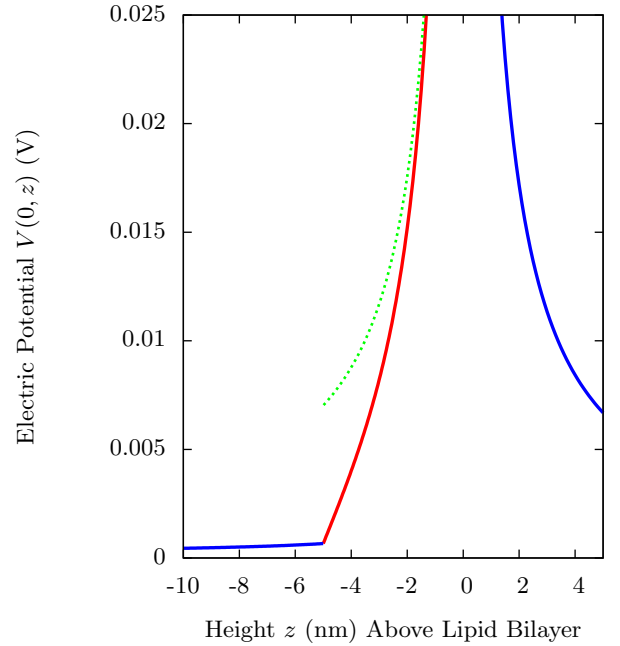


FIG. 1: The potentials (6–8) above, $V_w(0, z)$ (blue), and below, $V_\ell(0, z)$ (red) and $V_c(0, z)$ (blue), a unit charge $q = |e|$ at $(\rho, z) = (0, 0)$ are plotted for a lipid bilayer of thickness $t = 5$ nm. The green dotted curve follows the simple approximation (10).

In and near the extracellular region, these potentials are fairly well approximated by the simple formulas

$$V_w(0, z) \approx \frac{q}{4\pi\epsilon_0\epsilon_w} \left(\frac{1}{|z-h|} + \frac{p}{z+h} \right) \quad (9)$$

$$V_\ell(0, z) \approx \frac{q}{4\pi\epsilon_0\epsilon_w\ell |z-h|} \quad (10)$$

which hold when the lipid bilayer is infinitely thick. But the potential $V_\ell(0, z)$ drops significantly below the simple formula (10) as z descends deeper into the bilayer and nearly vanishes at the lipid-cytosol interface as does $V_c(0, z)$ in the cytosol.

For a unit charge $q = |e|$ at $(\rho, z) = (0, 0)$, the potentials (6–8) are plotted in Fig. 1: $V_w(0, z)$ (blue), $V_\ell(0, z)$ (red), and $V_c(0, z)$ (blue). The green dotted curve follows the simple approximation (10) to $V_\ell(0, z)$. The potential $V_\ell(0, -t)$ at the interface between the cytosol and the bilayer is 6.6×10^{-4} V, so that a unit charge there would have an electrostatic energy (due to the charge $|e|$ at $(0, 0)$) of only about $kT_b/40$ at body temperature.

Fig. 2 plots the potentials (6–8) due to a unit charge at $(\rho, z) = (0, 0)$ for lipid bilayers of thicknesses $t = 2, 3, 4,$ and 5 nm. Even for a bilayer as thin as 2 nm, the potential $V_c(0, -t)$ directly below the charge at the interface between the cytosol and the bilayer is less than a tenth of $kT_b/|e|$.

These potentials and figures illustrate the extraordinary electrostatic insulation provided by the lipid bilayer.

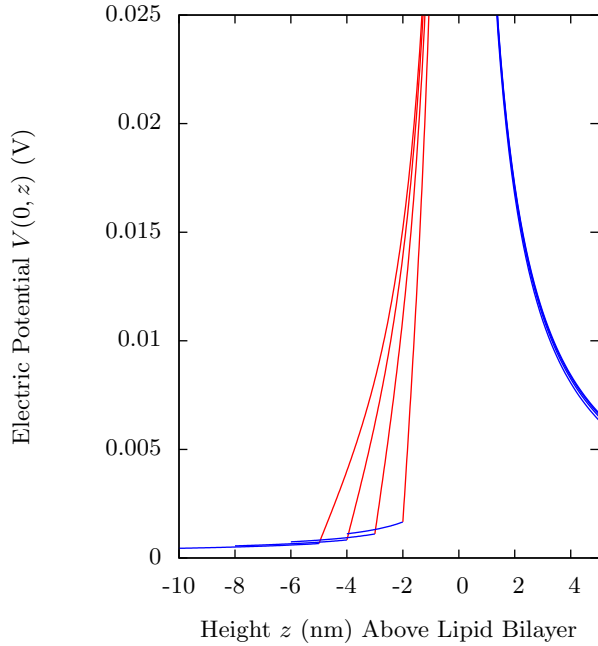


FIG. 2: The potentials (7, 6, & 8) above $V_w(0, z)$ (blue) and below $V_\ell(0, z)$ (red) and $V_c(0, z)$ (blue) a unit charge $q = |e|$ at $(\rho, z) = (0, 0)$ are plotted for lipid bilayers of thickness $t = 2, 3, 4,$ and 5 nm. Note that the potential at the interface between the cytosol and the bilayer is less than a tenth of kT even for a bilayer as thin as 2 nm.

VI. ELECTROPORATION MODEL

A. Electroporation

Somewhat paradoxically, the remarkable electrostatic insulation provided by the lipid bilayer makes membrane proteins more sensitive to charges lying outside the cell and also makes cells more vulnerable to electroporation. The reason for both of these effects is that the electric field \mathbf{E} in the lipid bilayer due to a charge q at the interface between the bilayer and the extracellular environment is

$$\mathbf{E} = -[V_\ell(0, 0) - V_\ell(0, -t)] \frac{\hat{z}}{t} \quad (11)$$

apart from the screening effects of counterions. Since even a charge $q = \pm 10e$ makes a potential $V_\ell(0, -t)$ at $z = -t$ that is less than $kT_b/|e|$, this electric field is approximately

$$\mathbf{E} \approx -V_\ell(0, 0) \frac{\hat{z}}{t} \quad (12)$$

which is larger than if the potential $V_\ell(0, -t)$ were more significant.

Electroporation is the formation of pores in membranes by an electric field. Depending on the duration of the field and the type of cell, an electric potential difference

TABLE I: The voltage differences $\Delta V_{CPP} + \Delta V_{NaCl}$ (mV) across the plasma membrane induced by an R^N oligoarginine as an α -helix, a random coil, or a β -strand and by the ions of 156 mM Na^+ and Cl^- reacting to it. The resting transmembrane potential $-120 < \Delta V_{cell} < -20$ mV is not included.

N	R^N α -helix	R^N random coil	R^N β -strand
5	-144 ± 4	-154 ± 3	-148 ± 4
6	-174 ± 4	-173 ± 4	-168 ± 1
7	-206 ± 4	-201 ± 3	-189 ± 2
8	-232 ± 3	-228 ± 1	-199 ± 5
9	-256 ± 6	-246 ± 2	-205 ± 4
10	-281 ± 2	-260 ± 5	-210 ± 4
11	-306 ± 5	-260 ± 3	-218 ± 4
12	-323 ± 4	-261 ± 4	-213 ± 2

across a cell's plasma membrane in excess of about 200 mV will create pores.

There are two main components to the energy of a pore. The first is the line energy $2\pi r\gamma$ due to the linear tension γ , which is of the order of 10^{-11} J/m. The second is the electrical energy $-0.5\Delta C\pi r^2(\Delta V)^2$ in which ΔV is the voltage across the membrane and $\Delta C = C_w - C_\ell$ is the difference between the specific capacity per unit area $C_w = \epsilon_w\epsilon_0/t$ of the water-filled pore and that $C_\ell = \epsilon_\ell\epsilon_0/t$ of the pore-free membrane of thickness t . There also is a small term due to the surface tension Σ of the plasma membrane of the cell, but this term usually is negligible since Σ is of the order of 2.5×10^{-6} J/m² [41]. The energy of the pore in a plasma membrane is then [42–46]

$$E(r) = 2\pi r\gamma - \pi r^2\Sigma - \frac{1}{2}\pi r^2\Delta C(\Delta V)^2. \quad (13)$$

This energy has a maximum of

$$E(r_c) = \frac{2\pi\gamma^2}{\Delta C(\Delta V)^2 + 2\Sigma} \approx \frac{2\pi\gamma^2}{\Delta C(\Delta V)^2} \quad (14)$$

at the critical radius

$$r_c = \frac{2\gamma}{\Delta C(\Delta V)^2 + 2\Sigma} \approx \frac{2\gamma}{\Delta C(\Delta V)^2}. \quad (15)$$

The chance of a pore forming rises steeply with the magnitude of the voltage and falls with the radius of the pore.

If the transmembrane potential ΔV is turned off before the radius of the pore reaches r_c , then the radius r of the pore usually shrinks quickly (well within 1 ms [43]) to a radius so small as to virtually shut-down the conductivity of the pore. This rapid closure occurs because in (13) the energy $2\pi r\gamma$ dominates over $-\pi r^2\Sigma$, the surface tension Σ being negligible. Such a pore is said to be reversible. But if ΔV remains on when r exceeds the critical radius r_c , then the pore usually will grow and lyse the cell; such a pore is said to be irreversible.

The formula (15) provides an upper limit on the radius of a reversible pore. This upper limit drops with the square of the transmembrane voltage ΔV from $r_c = 3.6$ nm for $\Delta V = -200$ mV, to 1.6 nm for $\Delta V = -300$, and to 0.9 nm for $\Delta V = -400$ mV.

The time t_ℓ for a pore's radius to reach the critical radius r_c is the time to lysis; it varies greatly and apparently randomly even within cells of a given kind. In erythrocytes, its mean value drops by nearly an order of magnitude with each increase of 100 mV in the transmembrane potential [43] and is about a fifth of a second when $\Delta V = -300$ mV.

The chance of a potential ΔV forming a pore of radius r is proportional to the Boltzmann factor $\exp(-E(r)/(kT))$. The higher the potential ΔV and the narrower the pore, the greater the chance of pore formation.

B. The Model

In the model advanced in references [4, 5], a polyarginine sticks to the cell membrane as its guanidinium groups electrostatically interact with the phosphate groups of the outer leaflet of the phospholipid bilayer. If the positive charge of the polyarginine exceeds about $8|e|$, then it can raise the transmembrane potential above the threshold for electroporation, some -200 mV [41–46].

The transmembrane potential ΔV is the sum of three terms

$$\Delta V = \Delta V_{cell} + \Delta V_{CPP} + \Delta V_{NaCl} \quad (16)$$

the resting transmembrane potential ΔV_{cell} of the cell in the absence of CPPs, the transmembrane potential ΔV_{CPP} due to an oligoarginine or other CPP, and the transmembrane potential ΔV_{NaCl} due to the counterions of the extracellular medium. The resting transmembrane potential ΔV_{cell} of the cell varies between about 20 mV to more than 70 mV, depending upon the type of cell. Ideally, it is measured experimentally. The transmembrane potential ΔV_{CPP} due to an oligoarginine or to some other positively charged CPP may be determined from the formulas (1–8) for the potential of a charge outside a membrane [4]. The transmembrane potential ΔV_{NaCl} due to the counterions of the extracellular medium requires a Monte Carlo simulation of the Na^+ , Cl^- , and other ions of the extracellular medium in the electrostatic potential $V_{cell} + V_{CPP}$. This simulation was performed in [4] with the aid of equations (1–8). The lipid bilayer insulates the extracellular counterions from the potential due to the counterions of the cytosol, however, so their potential may be neglected in the simulation of the extracellular counterions.

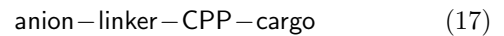
The values of $\Delta V_{CPP} + \Delta V_{NaCl}$ found in Monte Carlo simulations [4] of the salt around an R^N oligoarginine are listed in the table. A resting transmembrane potential $-120 < \Delta V_{cell} < -20$ mV should be added to these values of $\Delta V_{CPP} + \Delta V_{NaCl}$ to obtain the full transmembrane potential ΔV . For $N > 8$, the transmembrane potential ΔV can exceed -200 mV which is enough [41–46] to cause electroporation in common eukaryotic cells.

In references [5] and [4], it was pointed out that one way to test the model advanced in those papers would be to look for the formation of reversible pores by detecting transient (ms) changes in the conductance of membranes exposed to CPPs such as R^9 . Such experiments have now been done. Using the planar-phospholipid-bilayer method, Hecce *et al.* found that R^9 induced transient ionic currents through model phospholipid membranes [6]. They estimated that the mean radius of these pores to be 0.66 nm, which is safely below the limiting critical radius (15) of between 0.9 and 3.6 nm for the voltage range of $-400 \leq \Delta V \leq -200$ mV. Moreover, using the patch-clamp technique, they found that R^9 induced transient ionic currents through the membranes of both freshly isolated human umbilical-artery (HUA) smooth-muscle cells and cultured osteosarcoma cells [6]. These experimental confirmations of the predictions made in references [5] and [4] lend some support to the model advanced in these papers and sketched in this subsection, but they do not prove that it is correct. It is, in any case, a continuum model of a molecular effect, and it may be consistent with the one simulated in reference [6].

VII. SMART DRUGS

Oligoarginines and other cell-penetrating peptides can carry cargos of up to 4000 Da across the lipid bilayer of eukaryotic cells by molecular electroporation [4, 5]. This ability to transduce cargos that substantially exceed the nominal restriction barrier of 500 Da of the “rule of five” [3] makes possible therapies like those sketched in section III.

But we also need a way of targeting cancer cells. One way to do this has been suggested by Tsien [10]. His idea is to attach a negatively charged molecule, an anion, to the CPP-cargo molecule by a polypeptide linker that is cut primarily by peptidases that are over-expressed by the targeted cells. The geometry he proposed is



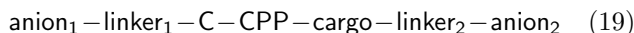
in which the hyphens represent covalent bonds. The cargo is the therapeutic compound. It might be one of the peptides of ([10]–[22]), which consisted of between 8 and 33 amino acids, or simply a cytotoxin. If the negative charge of the anion lowers total charge of the anion-linker-CPP-cargo molecule below a few $|e|$, then it will not enter the cell by transduction because, in the model [4, 5], its transmembrane potential ΔV will be too small to cause electroporation. (The anion-linker-CPP-cargo molecule might enter the cell by endocytosis, but then it would risk destruction as the pH of the endosome dropped to that of a lysosome.) Metastatic cancer cells over-express certain transmembrane peptidases. So to target them, one would pick a linker that is cut by one of these over-expressed transmembrane peptidases.

A. Better Geometries

One may improve the selectivity of such a smart drug by attaching two or more anions to the positively charged CPP-cargo by two or more *different* linkers that are cut primarily by *different* peptidases that are over-expressed by the targeted cells. A simple geometry for two anions and two different linkers is



To attach more than two anions by more than two different linkers, one can prepare an oxidizing solution of two classes of molecules. A simple example of a molecule of the first class is the molecule (18) with an extra cysteine (C)

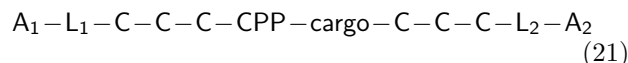


where the hyphens represent covalent bonds. Other examples of first-class molecules contain more cysteines to the left and/or right of the CPP-cargo moiety.

In a more compact notation in which A stands for an anion and L for a linker, two more examples of first-class molecules are



with four extra cysteines and



with six. First-class molecules must have their cysteines closer than any of the linkers to the CPP-cargo moiety; otherwise the cutting of a single linker could set adrift more than one anion.

Molecules of the second class consist of a cysteine covalently fused to a linker that in turn is covalently fused to an anion; that is, second-class molecules are of the form



in which L_k is a linker cleavable by a peptidase over-expressed by the target cells and A_k is an anion.

In an oxidizing solution of these two classes of molecules, a cysteine of a second-class molecule can form a disulfide bond with a cysteine in a first-class molecule. Thus, smart drugs can form in which three or more anions are fused to the CPP-cargo molecule by linkers that can be cut by peptidases over-expressed by the target cells. For instance, an oxidizing solution of the first-class molecule (19) and the second-class molecule (22) would make the smart drug shown in Fig. 3. Similarly, an oxidizing solution of the first-class molecule (20) and the second-class molecule (22) for $k = 3, 4, 5,$ and 6 would form the smart drug of Fig. 4.

Of course, undesirable disulfide bonds also would form. One way to suppress unwanted disulfide bonds is to titrate a dilute reducing solution of different second-class molecules (22) into an oxidizing solution of first-class

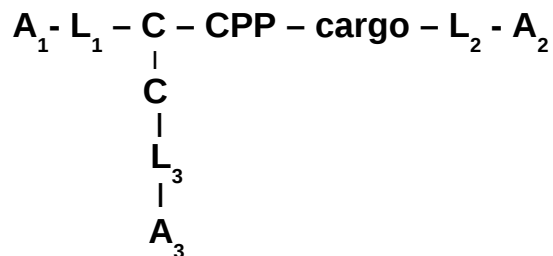


FIG. 3: A smart drug consisting of a CPP-cargo molecule and three anions fused to it by three different linkers that are cut primarily by peptidases over-expressed mainly by the targeted cells. Here **A**, **C**, and **L** respectively stand for anion, cysteine, and (8 aa) linker. The hyphens and vertical lines represent covalent bonds.

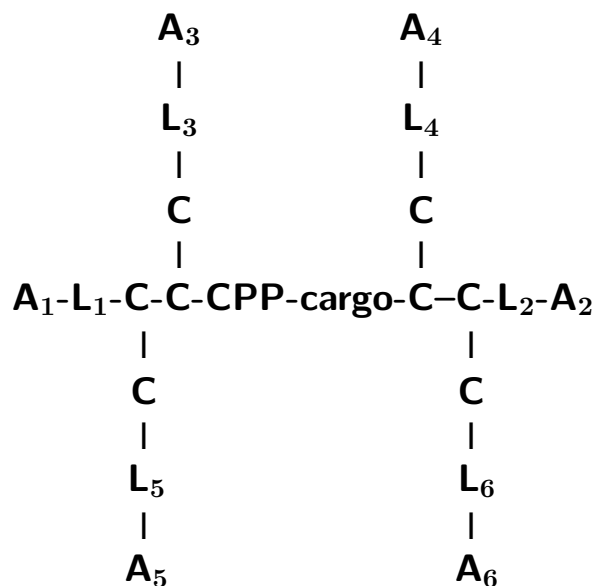


FIG. 4: A smart drug consisting of a CPP-cargo molecule and six anions fused to it by six different linkers that are cut primarily by peptidases over-expressed mainly by the targeted cells. **A**, **C**, **L**, hyphens, and vertical lines are as in Fig. 3.

molecules such as (19, 20, or 21). The order of the linkers and anions does not matter as long as they are different and are cut primarily by peptidases that are over-expressed mainly by the target cells.

To achieve maximum specificity, it is desirable that the negative charge of each anion reduce the positive charge of the CPP to $4|e|$ or less, for in this case, the CPP-cargo molecule is not transduced until all the linkers are

cleaved. Thus, if the CPP is the oligoarginine R⁹ with charge $9|e|$, then a smart drug like that in Fig. 4 would have six anions of charge $-5|e|$ for a total charge of $q = -21|e|$. Such smart drugs would be negatively charged.

By using well-chosen linkers, disulfide bonds, CPP's, and cell-penetrating molecules (CPM's) such as cationic lipids, one can make a very wide variety of smart drugs.

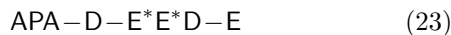
B. Linkers

Linkers are essential to the selectivity of the smart drugs sketched in this section. Each linker must be a short peptide that is cut primarily by a peptidase that is over-expressed mainly by the targeted cells.

MT1-MMP is a type-1 transmembrane proteinase essential for skeletal development, metastasis, and angiogenesis. The Burnham Institute's cut database [47] lists 37 eight-aa-long sequences that have been shown by experiment to be cut by MT1-MMP and that are not known to be cut by other human peptidases: PSQG-QKVE, NPMG-SEPV, GYFG-DPLA, NLAG-ILKE, GLRG-LQGP, LRRL-LGLF, AVEG-SGKS, DLSL-ISPL, LISP-LAQA, GEYR-TNPE, PSQG-QKVE, TKRD-LALS, RVLG-LETE, RLLG-LFGE, DPFR-LQCT, LPPG-LPLT, PPSY-LGDR, QLYG-GESG, NFFP-RKPK, DPSA-IMAP, QGLK-WQHN, FCIQ-NYTP, AEPW-TVRN, QQLY-GGES, PQPR-TTSR, AQLG-VMQG, MDET-MKEL, KAYK-SELE, LLLS-SDVN, LILS-DVND, DSHS-LTTN, LRGD-FSSA, NMID-AATL, KAIQ-LTYN, GLRG-LQGP, SSER-SSTS, and TSGG-YIFY. MT1-MMP cuts these 37 octapeptides at the hyphens. Although 37 sequences may seem so numerous as to be unselective, in fact, they are 37 out of $20^8 = 25,600,000,000$ possible 8-aa sequences.

The ADAMs are membrane proteins that have both a disintegrin domain and a metalloprotease domain. ADAM9, 10, 12, 15, and 17 have been found in cancer cells. ADAM17 (aka TACE) sheds and/or processes TNF α , TGF α , APP, amphiregulin, p75TNFR, p55TNFR, TRANCE, L-selectin, IL-6 receptor, IL-1 receptor II, Notch1 receptor, growth hormone-binding protein, MUC1, and transmembrane collagen XVII [48]. The Burnham cut database [47] lists nine eight-amino-acid-long sequences that have been shown by experiment to be cut by ADAM17 and that are not known to be cut by any other human peptidase: DLLA-VVAA, NSAR-SEGP, KLDK-SFSM, LPVQ-DSSS, WTGH-STLP, RLRR-GLAA, KSMK-THSM, RVEQ-VVKP, and VAAA-VVSH. The cuts occur at the hyphens.

Prostate-specific membrane antigen (PSMA) is a glutamate carboxypeptidase II highly expressed by prostate epithelial cells and by the neovasculature of many tumor types but not by endothelial cells in normal tissue [49]. Denmeade *et al.* have found [49] that the substrate



is stable in blood but is cut—at the second hyphen—by PSMA. Here APA is 4-N[N-2,4diamino-6-pteridinyl-

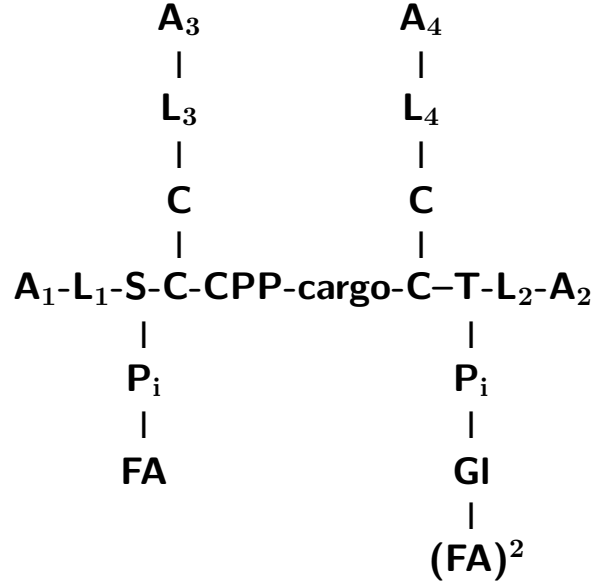


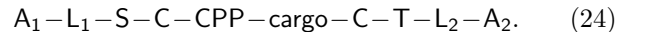
FIG. 5: A smart drug consisting of a CPP-cargo molecule and four anions fused to it by four different linkers that are cut primarily by peptidases over-expressed mainly by the targeted cells. \mathbf{P}_i stands for inorganic phosphate, \mathbf{FA} for fatty acid, and \mathbf{GI} for glycerol. \mathbf{A} , \mathbf{C} , \mathbf{L} , hyphens, and vertical lines are as in Fig. 3.

methyl)-N-methylamino-benzoate], and the asterisks represent γ -linkages, while the hyphens stand for the usual α -linkages.

C. Cell-Penetrating Molecules

Two features of oligoarginines allow them to penetrate through cell membranes: a positive charge exceeding $8|e|$ and several guanidinium groups. Thus any molecule with several guanidinium groups and a positive charge exceeding $8|e|$ may be as good a cell-penetrating molecule (CPM) as the oligoarginines considered in this paper.

Cationic lipids can penetrate cell membranes; they form another category of cell-penetrating molecules. One design for a cationic lipid has one or several serines \mathbf{S} and/or threonines \mathbf{T} to the left and/or right of the CPP-cargo moiety. Thus an example of a first-class molecule for a cationic-lipid CPM is



To complete this first-class molecule one would use the same kind (22) of second-class molecule and third-class molecules that are either a fatty acid \mathbf{FA} fused to an inorganic phosphate group \mathbf{P}_i by an acyl-phosphate bond



or a phospholipid without its polar head group

$$(FA)^2 = GI - P_i \quad (26)$$

in which GI is a glycerol. One would make the cationic-lipid CPM by fusing the second-class molecules to the cysteines C by disulfide bonds and the third-class molecules to the hydroxyl groups of serines S and threonines T by ester bonds. The resulting smart drug is illustrated in Fig. 5. Such cationic-lipid smart drugs with various numbers of anions, linkers, and lipids may be able to carry therapeutic cargos across the cell membrane.

D. Stability

Blood has peptidases that cut peptides and RNAses that cut RNAs, but there are some biochemical tricks that can increase the stability of peptides and RNAs in smart drugs. One may use right-handed amino acids to frustrate peptidases. A peptide made of right-handed amino acids in reverse order can have similar biochemical properties to its normally ordered left-handed twin [1]. Such *retro-inverso* peptides are more stable in the body and were used in several of the therapeutic experiments sketched in section III. RNAs made with 2'-*O*-methyl-modified nucleotides with phosphorothioate linkages resist RNAses [50]. The wide class of cell-penetrating molecules may have members that are stable in the human body and unlikely to stimulate an immune response.

E. Ligands and Antibodies

What is really needed for specificity is knowledge of what distinguishes the surface of a cancer cell from that of a healthy cell. Cancer cells over-express many receptors, such as the CXC chemokine receptor 4 (CXCR4), the specific neurokinin-1 (NK-1) receptor, folate receptors (FRs), the G-protein-coupled protease-activated receptor PAR-1, and receptors for many regulatory peptides. Metastatic cancer cells over-express many trans-membrane peptidases. A reasonably complete characterization of the distinguishing features of the surfaces of cancer cells would advance the development of compounds that bind to these features. Such an artificial feature-ligand (FL) could guide a CPP-cargo molecule

to cancer cells. The simplest geometry would be

$$FL - L_1 - CPP - \text{cargo} - L_2 - A \quad (27)$$

in which the linkers L_1 and L_2 are cleavable by peptidases overexpressed by the cancer cell that overexpresses the feature F .

VIII. SUMMARY

In a model, which recently has received some experimental support, polyarginines carry cargos by molecular electroporation across the cell membrane. They and other cell-penetrating peptides (CPPs) as well as cell-penetrating molecules (CPMs), such as cationic lipids, can transduce therapeutic cargos that greatly exceed the 500 Da restriction barrier. They may solve part of the drug-delivery problem.

The use of well chosen linkers and anions can help target cancer cells and spare healthy ones. The development of really smart drugs, however, requires a more complete characterization of the differences between the surfaces of cancer cells and those of normal cells.

Acknowledgments

I am grateful to Leonid Chernomordik for tips about electroporation, to Gisela Tünnemann for sharing her data, to Sergio Hassan for advice about the NaCl potential, to Pavel Jungwirth for advice on guanidinium groups, to John Connor and Karlheinz Hilber for explaining the status of measurements of the membrane potential of mouse myoblast cells, to Paul Robbins for sending me some of his images, and to Jean Vance for information about mammalian cells deficient in the synthesis of phosphatidylserine. Thanks also to S. Atlas, B. Becker, H. Berg, S. Bezrukov, H. Bryant, P. Cahill, D. Cromer, E. Evans, A. E. Garcia, B. Goldstein, G. Herling, T. Hess, S. Koch, V. Madhok, M. Malik, A. Parsegian, B. B. Rivers, K. Thickman, T. Tolley, and J. Thomas for useful conversations, and to K. Dill, S. Dowdy, S. Henry, K. Hilber, A. Pasquinelli, B. Salzberg, D. Sergatskov, L. Sillerud, B. Smith, A. Strongin, R. Tsien, J. Vance, and A. Ziegler for helpful e-mail.

-
- [1] Chorev, M., and M. Goodman, 1993. A dozen Years of Retro-Inverso Peptidomimetics. *Acc. Chem. Res.* 26(5):266 – 273.
- [2] Manoharan, M., V. Kesavan, and K. G. Rajeev, 2005. SiRNAs containing ribose substitutes to which lipophilic moieties may be attached. *U. S. Pat. Appl. Publ.* US:2005107325.
- [3] Lipinski, C., F. Lombardo, B. Dominy, and P. Feeney,

1997. Experimental and computational approaches to estimate solubility and permeability in drug discovery and development settings. *Adv. Drug Deliv. Rev.* 23:3–25.
- [4] Cahill, K. E., 2010. Molecular Electroporation and the Transduction of Oligoarginines. *Phys. Biol.* 7:016001(14pp).
- [5] Cahill, K. E., 2009. Simple model of the transduction of

- cell-penetrating peptides. *IET Syst. Biol.* 3(5):300–306.
- [6] Herce, H. D., A. E. Garcia, J. Litt, R. S. Kane, P. Martin, N. Enrique, A. Rebolledo, and V. Milesi, 2009. Arginine-Rich Peptides Destabilize the Plasma Membrane, Consistent with a Pore Formation Translocation Mechanism of Cell-Penetrating Peptides. *Biophys. J.* 97(7):1917–1925.
- [7] Green, M., and P. M. Loewenstein, 1988. Autonomous functional domains of chemically synthesized human immunodeficiency virus tat trans-activator protein. *Cell* 55(6):1179–1188.
- [8] Frankel, A. D., and C. O. Pabo, 1988. Cellular uptake of the tat protein from human immunodeficiency virus. *Cell* 55(6):1189–1193.
- [9] Lindberg, M., J. Jarvet, Ü. Langel, and A. Gräslund, 2001. Secondary Structure and Position of the Cell-Penetrating Peptide Transportan in SDS Micelles As Determined by NMR. *Biochemistry* 40(10):3141–3149.
- [10] Jiang, T., E. S. Olson, Q. T. Nguyen, M. Roy, P. A. Jennings, and R. Y. Tsien, 2004. Tumor imaging by means of proteolytic activation of cell-penetrating peptides. *Proc. Natl. Acad. Sci. USA* 101(51):17867–17872.
- [11] Snyder, E., C. Saenz, C. Denicourt, B. Meade, X. Cui, I. Kaplan, and S. Dowdy, 2005. Enhanced targeting and killing of tumor cells expressing the CXCR4 chemokine receptor 4 by transducible anticancer peptides. *Cancer Res.* 65(23):10646–50.
- [12] Willam, C., N. Masson, Y.-M. Tian, S. A. Mahmood, M. I. Wilson, R. Bicknell, K.-U. Eckardt, P. H. Maxwell, P. J. Ratcliffe, and C. W. Pugh, 2002. Peptide blockade of HIF α degradation modulates cellular metabolism and angiogenesis. *Proc. Natl. Acad. Sci.* 99(16):10423–10428.
- [13] Chen, Y.-N. P., S. K. Sharma, T. M. Ramsey, L. Jiang, M. S. Martin, K. Baker, P. D. Adams, K. W. Bair, and W. G. Kaelin Jr., 1999. Selective killing of transformed cells by cyclin/cyclin-dependent kinase 2 antagonists. *Proc. Natl. Acad. Sci. USA* 96(8):4325–4329.
- [14] Mendoza, N., S. Fong, J. Marsters, H. Koeppen, R. Schwall, and D. Wickramasinghe, 2003. Selective Cyclin-dependent Kinase 2/Cyclin A Antagonists that Differ from ATP Site Inhibitors Block Tumor Growth. *Cancer Res.* 63(5):1020–1024.
- [15] Harbour, J. W., L. Worley, D. Ma, and M. Cohen, 2002. Transducible peptide therapy for uveal melanoma and retinoblastoma. *Arch. Ophthalmol.* 120(10):1341–1346.
- [16] Mai, J. C., Z. Mi, S.-H. Kim, B. Ng, and P. D. Robbins, 2001. A Proapoptotic Peptide for the Treatment of Solid Tumors. *Cancer Res.* 61 (21):7709–7712.
- [17] Datta, K., C. Sundberg, S. A. Karumanchi, and D. Mukhopadhyay, 2001. The 104–123 Amino Acid Sequence of the β -domain of von Hippel-Lindau Gene Product Is Sufficient to Inhibit Renal Tumor Growth and Invasion. *Cancer Res.* 61 (5):1768–1775.
- [18] Hosotani, R., Y. Miyamoto, K. Fujimoto, R. Doi, A. Otaka, N. Fujii, and M. Imamura, 2002. Trojan p16 Peptide Suppresses Pancreatic Cancer Growth and Prolongs Survival in Mice. *Clin. Cancer Res.* 8(4):1271–1276.
- [19] Zhou, J., J. Fan, and J.-T. Hsieh, 2006. Inhibition of Mitogen-Elicited Signal Transduction and Growth in Prostate Cancer with a Small Peptide Derived from the Functional Domain of DOC-2/DAB2 Delivered by a Unique Vehicle. *Cancer Res.* 66(18):8954–8958.
- [20] Snyder, E., B. Meade, C. Saenz, and S. Dowdy, 2004. Treatment of Terminal Peritoneal Carcinomatosis by a Transducible p53-Activating Peptide. *PLoS Biology* 2(2):0186–0193.
- [21] Haase, H., G. Dobbernack, G. Tünnemann, P. Karczewski, M. C. Cardoso, D. Petzhold, W. P. Schlegel, S. Lutter, P. Pierschalek, J. Behlke, and I. Morano, 2006. Minigenes encoding N-terminal domains of human cardiac myosin light chain-1 improve heart function of transgenic rats. *FASEB J* 20 (7):865–873.
- [22] Tünnemann, G., P. Karczewski, H. Haase, M. C. Cardoso, and I. Morano, 2007. Modulation of muscle contraction by a cell-permeable peptide. *J Mol Med* 85(12):1405–1412.
- [23] Ziegler, A., and J. Seelig, 2007. High Affinity of the Cell-Penetrating Peptide HIV-1 Tat-PTD for DNA. *Biochemistry* 46(27):8138–45.
- [24] Tünnemann, G., R. M. Martin, S. Haupt, C. Patsch, F. Edenhofer, and M. C. Cardoso, 2006. Cargo-dependent mode of uptake and bioavailability of TAT-containing proteins and peptides in living cells. *FASEB J* 20 (11):1775–1784.
- [25] Wadia, J. S., R. V. Stan, and S. F. Dowdy, 2004. Transducible TAT-HA fusogenic peptide enhances escape of TAT-fusion proteins after lipid raft macropinocytosis. *Nat. Med.* 10(3):310–315.
- [26] Duchardt, F., M. Fotin-Mleczek, H. Schwarz, R. Fischer, and R. Brock, 2007. A Comprehensive Model for the Cellular Uptake of Cationic Cell-penetrating Peptides. *Traffic* 8(7):848–866.
- [27] Prochiantz, A., 2000. Messenger proteins: homeoproteins, TAT and others. *Curr Opin Cell Biol* 12(4):400–406.
- [28] Dom, G., C. Shaw-Jackson, C. Matis, O. Bouffieux, J. J. Picard, A. Prochiantz, M.-P. Mingeot-Leclercq, R. Bresseur, and R. Rezsöházy, 2003. Cellular uptake of Antennapedia Penetratin peptides is a two-step process in which phase transfer precedes a tryptophan-dependent translocation. *Nucleic Acids Res* 31(2):556–561.
- [29] Rothbard, J. B., T. C. Jessop, and P. A. Wender, 2005. Adaptive translocation: the role of hydrogen bonding and membrane potential in the uptake of guanidinium-rich transporters into cells. *Adv. Drug Delivery Rev.* 57(4):495–504.
- [30] Zaro, J. L., and W.-C. Shen, 2005. Evidence that membrane transduction of oligoarginine does not require vesicle formation. *Exp. Cell Res.* 307:164–173.
- [31] Ziegler, A., P. Nervi, M. Dürrenberger, and J. Seelig, 2005. The Cationic Cell-Penetrating Peptide CPP^{TAT} Derived from the HIV-1 Protein TAT Is Rapidly Transported into Living Fibroblasts: Optical, Biophysical, and Metabolic Evidence. *Biochemistry* 44(1):138–148.
- [32] Patel, L. N., J. L. Zaro, and W.-C. Shen, 2007. Cell Penetrating Peptides: Intracellular Pathways and Pharmaceutical Perspectives. *Pharmaceutical Research* 24(11):1977–1992.
- [33] Fawell, S., J. Seery, Y. Daikh, C. Moore, L. Chen, B. Pepinsky, and J. Barsoum, 1994. Tat-mediated delivery of heterologous proteins into cells. *Proc. Natl. Acad. Sci. USA* 91:664.
- [34] Nagahara, H., A. Vocero-Akbani, E. Snyder, A. Ho, D. Latham, N. Lissy, M. Becker-Hapak, S. Ezhevsky, and S. Dowdy, 1998. Transduction of full-length TAT fusion proteins into mammalian cells: TAT-p27^{Kip1}. *Nature Medicine* 4:1449.

- [35] Bulte, J. W., 2006. Intracellular endosomal magnetic labeling of cells. *Methods in Molecular Medicine* 124:419.
- [36] Garden, O., P. Reynolds, J. Yates, D. Larkman, F. Marelli-Berg, D. Haskard, A. Edwards, and A. George, 2006. A rapid method for labelling CD4⁺ T cells with ultrasmall paramagnetic iron oxide nanoparticles for magnetic resonance imaging that preserves proliferative, regulatory and migratory behaviour *in vitro*. *J. Immunol. Methods* 314:123–133.
- [37] Tünnemann, G., G. Ter-Avetisyan, R. M. Martin, M. Martin Stöckl, A. Herrmann, and M. C. Cardoso, 2008. Live-cell analysis of cell penetration ability and toxicity of oligo-arginines. *J. Peptide Science* 14(4):469–76.
- [38] Bevers, E., P. Comfurius, D. Dekkers, and R. Zwaal, 1999. Lipid translocation across the plasma membrane of mammalian cells. *Biochim Biophys Acta* 1439(3):317–30.
- [39] Alberts, B., A. Johnson, J. Lewis, M. Raff, K. Roberts, and P. Walter, 2002. *Molecular Biology of the Cell*, Garland Science, New York, 587–593. 4 edition.
- [40] Tyagi, M., M. Rusnati, M. Presta, and M. Giacca, 2001. Internalization of HIV-1 Tat Requires Cell Surface Heparan Sulfate Proteoglycans. *J. Biol. Chem.* 276(5):3254–3261.
- [41] Dai, J., H. P. Ting-Beall, and M. P. Sheetz, 1997. The Secretion-coupled Endocytosis Correlates with Membrane Tension Changes in RBL 2H3 Cells. *J. Gen. Physiol.* 110(1):1–10.
- [42] Abidor, I. G., V. B. Arakelyan, L. V. Chernomordik, Y. A. Chizmadzhev, V. F. Pastushenko, and M. R. Tarasevich, 1979. Electric Breakdown of Bilayer Lipid Membranes I. The Main Experimental Facts and Their Qualitative Discussion. *Bioelectrochem. Bioenerg.* 6:37–52.
- [43] Chernomordik, L. V., S. I. Sukharev, S. V. Popov, V. F. Pastushenko, A. V. Sokirko, I. G. Abidor, and Y. A. Chizmadzhev, 1987. The electrical breakdown of cell and lipid membranes: the similarity of phenomenologies. *Bioch. Biophys. Acta* 902:360–373.
- [44] Glaser, R. W., S. L. Leikin, L. V. Chernomordik, V. F. Pastushenko, and A. V. Sokirko, 1988. Reversible electrical breakdown of lipid bilayers: formation and evolution of pores. *Bioch. Biophys. Acta* 940:275–287.
- [45] Weaver, J., and Y. Chizmadzhev, 1996. Theory of electroporation: A review. *Bioelectrochemistry and Bioenergetics* 41:135–160. [http://dx.doi.org/10.1016/S0302-4598\(96\)05062-3](http://dx.doi.org/10.1016/S0302-4598(96)05062-3).
- [46] Melikov, K. C., V. A. Frolov, A. Shcherbakov, A. V. Samsonov, Y. A. Chizmadzhev, and L. V. Chernomordik, 2001. Voltage-Induced Nonconductive Pre-Pores and Metastable Single Pores in Unmodified Planar Lipid Bilayers. *Biophys. J.* 80:1829–1836.
- [47] Burnham. [Http://cutdb.burnham.org/](http://cutdb.burnham.org/).
- [48] Duffy, M. J., D. J. Lynn, A. T. Lloyd, and C. M. O’Shea, 2003. The ADAMs family of proteins: from basic studies to potential clinical applications. *Thrombosis and Haemostasis* 89(4):622–631.
- [49] Mhaka, A., A. M. Gady, K.-M. Lo, S. D. Gillies, and S. R. Denmeade, 2004. Use of Methotrexate-Based Peptide Substrates to Characterize the Substrate Specificity of Prostate-Specific Membrane Antigen (PSMA). *Cancer Biology & Therapy* 3:551–558.
- [50] Krutzfeldt, J., N. Rajewsky, R. Braich, K. G. Rajeev, T. Tuschl, M. Manoharan, and M. Stoffel, 2005. Silencing of microRNAs in vivo with ‘antagomirs’. *Nature* 438:685–689.